Oncogene (2004) 23, 267–277

www.nature.com/onc

Mapping and characterization of the minimal internal ribosome entry segment in the human c-*myc* mRNA 5′ untranslated region

Sabrina Cencig[1], Cécile Nanbru[1,3], Shu-Yun Le[2], Cyril Gueydan[1], Georges Huez[1] and Véronique Kruys*[,1]

[1]*Laboratoire de Chimie Biologique, Institut de Biologie et de Médecine Moléculaires, Université Libre de Bruxelles, rue des Profs Jeener et Brachet 12, 6041 Gosselies, Belgium;* [2]*Laboratory of Experimental and Computational Biology, NCI Center for Cancer Research, National Cancer Institute, NIH Frederick, USA*

The human c-*myc* proto-oncogene is transcribed from four alternative promoters generating transcripts with 5′ untranslated regions of various lengths. These transcripts encode two proteins, c-Myc1 and c-Myc2, from two initiation codons, CUG and AUG, respectively. We and others have previously demonstrated that the region of c-*myc* transcripts between nucleotides (nt) –363 and –94 upstream from the CUG start codon contained an internal ribosome entry site leading to the cap-independent translation of c-*myc* open reading frames (ORFs). Here, we mapped a 50-nt sequence (−143 −94), which is sufficient to promote internal translation initiation of c-*myc* ORFs. Interestingly, this 50-nt element can be further dissected into two segments of 14 nt, each capable of activating internal translation initiation. We also demonstrate that this 50-nt element acts as the ribosome landing site from which the preinitiation ribosomal complex scans the mRNA until the CUG or AUG start codons.
Oncogene (2004) **23,** 267–277. doi:10.1038/sj.onc.1207017

Keywords: translation; IRES; proto-oncogene; c-*myc*

Introduction

The c-*myc* proto-oncogene encodes a transcription factor which regulates the expression of many genes involved in the control of cell proliferation, differentiation and apoptosis (Ryan and Birnie, 1996; Obaya *et al*., 1999). c-*myc* gene expression is controlled at many levels (Marcu *et al*., 1992; Willis, 1999). In human, it can be transcribed from four alternative promoters P0, P1, P2, and P3, the latter one being located in the first intron of the gene (Bentley and Groudine, 1986a, b; Spencer *et al*., 1990). P1 and P2 are the two most commonly used promoters, together accounting for approximately 90% of c-*myc* transcripts in normal cells. The translation of these c-*myc* transcripts can be initiated at least at two different initiation codons (CUG or AUG) leading to the synthesis of two proteins (c-Myc1 and c-Myc2) (Hann *et al*., 1988) with distinct roles in the control of cell proliferation (Hann *et al*., 1992, 1994; Blackwood *et al*., 1994). Using the dicistronic vector assay, we and others have previously demonstrated the presence of an internal ribosome entry site (IRES) in P2 mRNA 5′ untranslated region (UTR). This element promotes cap-independent translation of c-Myc1/c-Myc2 open reading frames (ORFs) (Nanbru *et al*., 1997; Stoneley *et al*., 1998). It was further reported that c-*myc* mRNA remains associated with polysomes under conditions in which cap-dependent translation is inhibited, indicating that c-*myc* IRES is functional in its natural context (Johannes and Sarnow, 1998). Moreover, c-*myc* IRES activity is observed in apoptotic cells, during the G2/M transition of the cell cycle and upon genotoxic stress, conditions in which cap-dependent translation is severely impaired (Pyronnet *et al*., 2000; Stoneley *et al*., 2000; Subkhankulova *et al*., 2001). *In vivo*, the c-*myc* IRES is mainly active during embryogenesis, and is downregulated at later stages of development (Créancier *et al*., 2001).

Originally discovered in messenger RNAs from picornaviruses (Jackson, 1988; Pelletier and Sonenberg, 1988), IRESes are also found in cellular mRNAs. A cDNA microarray analysis of polysome-associated mRNAs at reduced eIF4F concentrations revealed that 200 out of 7000 genes analysed remain translationally active under these conditions (Johannes *et al*., 1999). This study thus suggests that IRES-mediated translation is clearly not a marginal alternative translation initiation pathway but conditions gene expression under several circumstances. Most cellular messenger RNAs containing an IRES are characterized by long and structured 5′ UTRs (e.g. IGF-II, VEGF, PDGF, Xiap, DAP5, PITSLRE mRNAs) (Teerink *et al*., 1995; Bernstein *et al*., 1997; Akiri *et al*., 1998; Huez *et al*., 1998; Holcik *et al*., 1999; Sella *et al*., 1999; Cornelis *et al*., 2000; Henis-Korenblit *et al*., 2000). These IRES differ in their primary sequences, but display some similarities in their secondary structures that appear to be crucial for their activity (Le and Maizel, 1997). Interestingly, internal ribosome entry can also be promoted by short

*Correspondence: V Kruys; E-mail: vkruys@ulb.ac.be
[3]Current address: Centre d'Etude et de Recherches Vétérinaires et Agrochimiques, 1180 Bruxelles, Belgium
Received 14 May 2003; revised 8 July 2003; accepted 8 July 2003

motifs. Indeed, a 9-nt sequence present in *Gtx* mRNA 5′UTR has been shown to mediate internal translation initiation (Chappell *et al*., 2000).

In this study, we report that the IRES promoting c-Myc1 and c-Myc2 translation consists in a short sequence element of 50 nt that recruits the translation preinitiation complex.

Results

*Prediction of c-*myc *IRES secondary structure and mapping of the IRES region*

Before mapping c-*myc* IRES, we determined a predictive secondary structure of the c-*myc* P2 5′ UTR. The RNA structure computed in human c-myc 5′UTR (accession number is V00568) is supported by phylogenetical analysis including 18 c-*myc* sequences. The predicted structure is characterized by a high degree of foldback and can be divided into three structural domains: domain A (−362 −285) which is engaged in a long-stem structure (−338 −285 and −106 −14), domain B which corresponds to a Y-shaped structure (−284 −144), including stems B1, B2 and B3 followed immediately by a small stem-loop B4 (−143 −106) and domain C (−105 −1) containing two hairpin structures (C1 and C2) in tandem and a single-stranded sequence stretch (−10 −2) that can be complementary to 18S rRNA 3′ end sequence (Figure 1). Interestingly, the Y-shaped structure and the following stem-loop of domain B reveal a common structural feature observed in several cellular IRES (Le and Maizel, 1997).

Based on this predictive structure, we performed a deletion analysis of c-*myc* P2 5′UTR to identify domains important for the IRES activity. In this purpose, we generated dicistronic DNA constructs containing as first ORF the sequence encoding CAT and as second ORF the sequence encoding a Myc-CAT fusion (BI) (Nanbru *et al*., 1997). This type of construct allows the simultaneous measurement of the expression of both cistrons exactly in the same experimental conditions, thereby providing a reliable comparison between cap-dependent and IRES-dependent translation initiation. c-*myc* P2 5′ UTR lacking different domains predicted by the computational analysis was inserted into the intercistronic region of these constructs. Moreover, the same P2 5′ UTR regions were inserted into a dicistronic construct containing a stable hairpin structure upstream the first cistron to block cap-dependent translation initiation (HP) (see Figure 2a, b). The different dicistronic constructs were transiently transfected in HeLa cells and the expression of the two cistrons was compared by Western immunoblotting with an

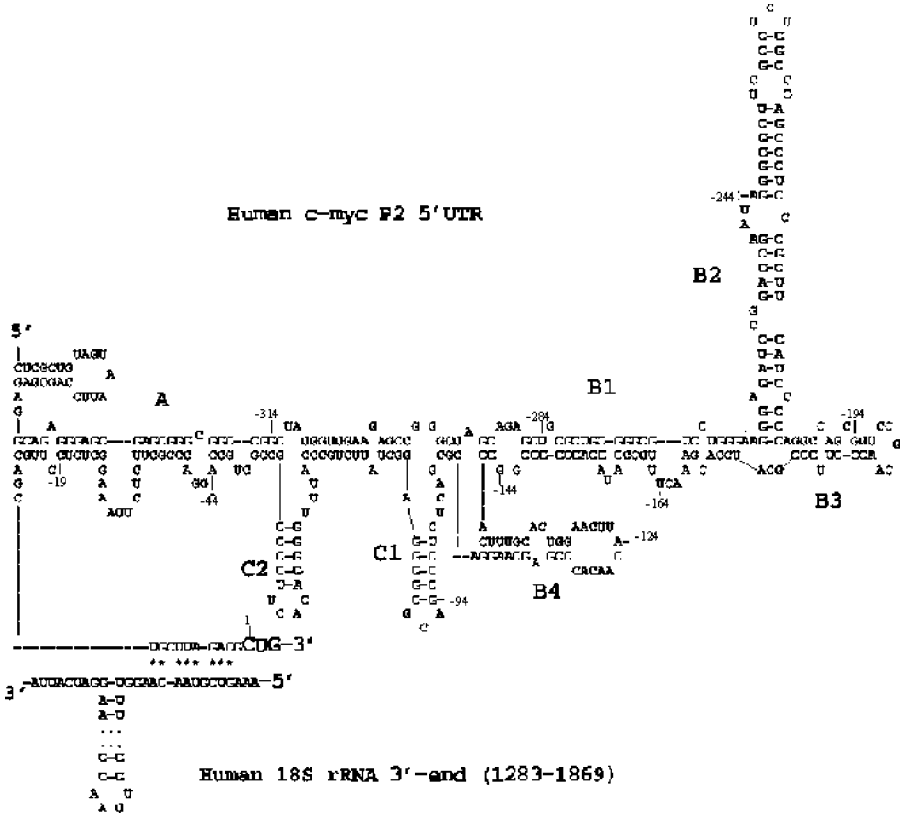

Figure 1 Secondary structure prediction of the c-*myc* P2 RNA leader (363 nt, CUG initiation codon: +1) was computed by the algorithm of Le and Maizel (1997) and mfold (Mathews *et al*., 1999). The structural domains are labelled by the stem A, Y-shaped structure (B1, B2 and B3), stem-loop B4 and two hairpin structures C1 and C2. The CUG initiation codon is indicated by the larger font. The sequence complementary to 18S rRNA 3′ end is indicated

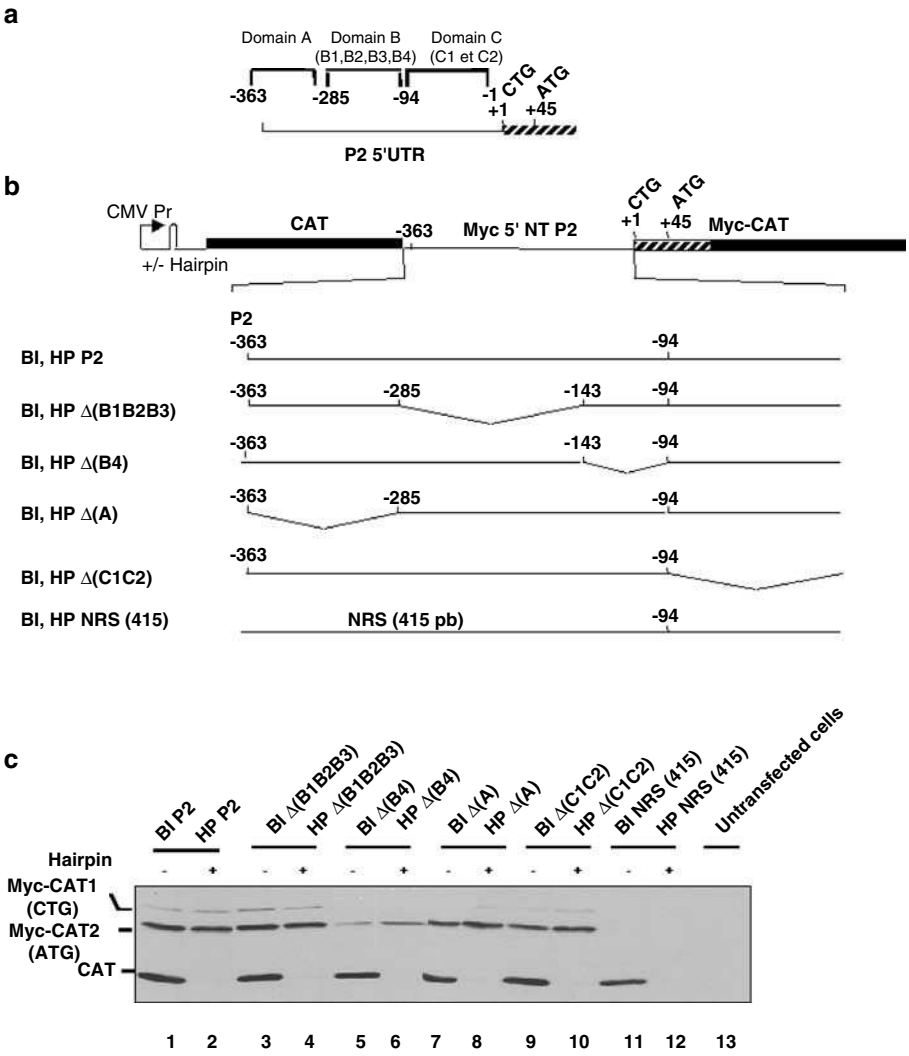

Figure 2 c-*myc* P2 IRES mapping by deletion of the different domains. (**a**) Schematic representation of the c-*myc* P2 mRNA 5′UTR. (**b**) Schematic representation of the dicistronic DNA constructs used for transfection experiments. The different c-*myc* leaders were fused to the CAT coding sequence (143 nt downstream from ATG codon) with the two initiation codons CTG and ATG of c-*myc* in frame with the CAT ORF. This fusion gives rise to chimeric Myc-CAT proteins of 32 kDa (ATG/Myc-CAT2) and 34 kDa (CTG/Myc-CAT1) as verified by specific mutation of the ATG or CTG initiation codons (data not shown). The chimeric Myc-CAT constructs were subcloned downstream from the CAT coding sequence under the control of the CMV promoter. The resulting plasmids (pBI MyCAT) encode dicistronic mRNAs bearing two tandem CAT ORFs of different lengths. The pHP MyCAT DNAs are derived from the pBI DNAs with the addition of a 5′-hairpin ($\Delta G = -40$ kcal/mol). The sizes of the different intercistronic regions inserted between CAT and Myc-CAT are indicated, nucleotide numbering starting at the CUG initiation codon. P2 includes the 363 nt of P2 leader. Δ(A), Δ(B1B2B3), Δ(B4) and Δ(C1C2) correspond to the P2 region lacking the domain A (−363 −285 nt), B1B2B3 (−284 −143 nt), B4 (−142 −94 nt) and C1C2 (−93 −1 nt), respectively. NRS(415) is a control sequence corresponding to 415 nt of TNF 3′ UTR region fused with the 95-nt long sequence localized upstream from c-*myc* CUG initiation codon. (**c**) HeLa cells were transfected with the dicistronic vectors described in (**b**) and the expression of the different constructs was analysed by Western immunoblotting using an anti-CAT antibody allowing the simultaneous detection of both ORF products (CAT and Myc-CAT). The same amount of protein extract was loaded on the gel. The names of the transfected plasmids, the presence (+) or the absence (−) of a hairpin in the constructs, and the CAT, Myc-CAT1, Myc-CAT2 products are indicated. The figure is representative of at least three independent experiments

anti-CAT antibody. As previously observed, c-myc P2 5′UTR promotes internal initiation of the second ORF at a rate of approximately one-fourth to one-third of the cap-dependent translation of the first cistron (mean value: 0.27 ± 0.07, see Materials and methods). Interestingly, only the deletion of domain B4 led to a significant decrease of c-*myc* IRES activity. Indeed, removal of the other domains (A, B1B2B3, C1C2) did not affect internal initiation of Myc-CAT ORF. These observations indicated that the B4 sequence is a major element of c-*myc* 5′ UTR for IRES activity.

In order to determine whether B4 was sufficient for IRES activity, we generated dicistronic constructs in which B4 alone or flanked by domain C was inserted in the intercistronic region of both BI and HP constructs (Figure 3a). The IRES activity of the inserted sequence was assayed as described above. This experiment revealed that B4 is sufficient to promote internal

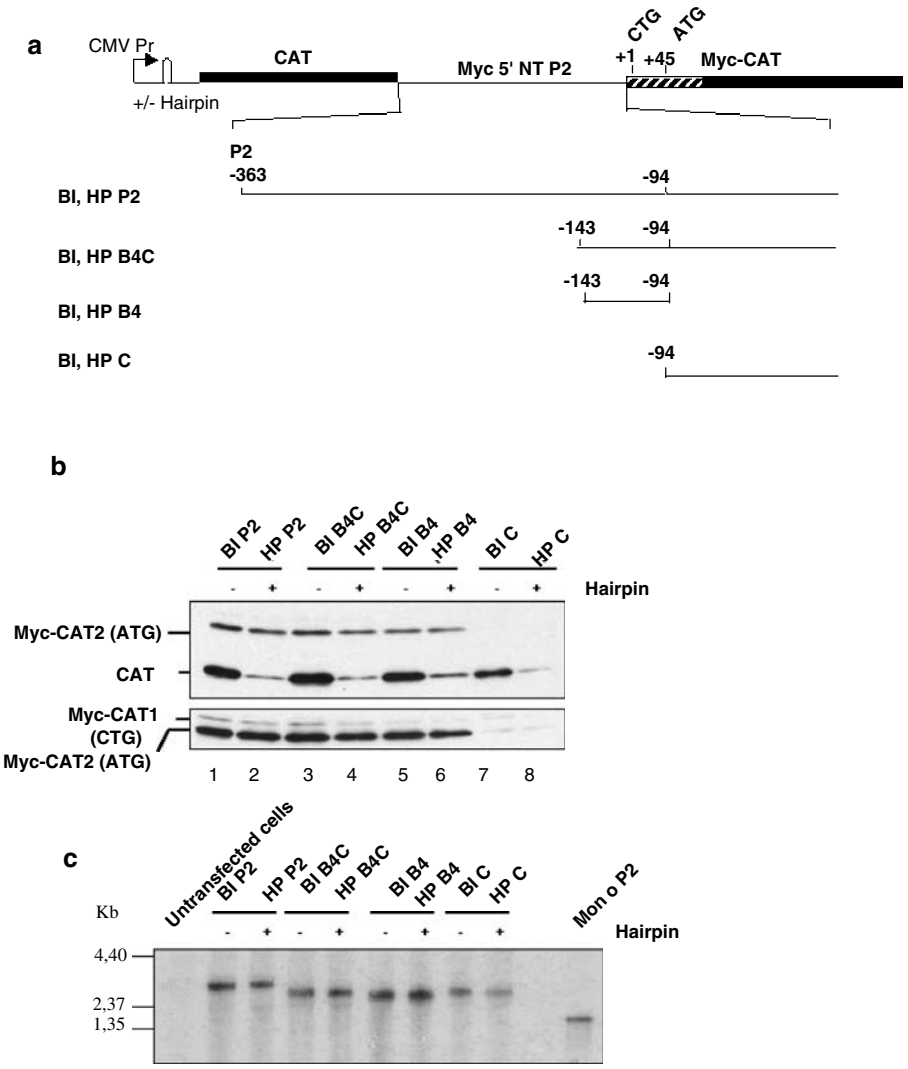

Figure 3 IRES activity of B4 sequence. (**a**) Schematic representation of the dicistronic DNA constructs used for transfection experiments. P2 was described in Figure 2. B4C, B4 and C contain the −143 −1 nt, −143 −94 nt and −94 −1 nt of the P2 region, respectively. (**b**) HeLa cells were transfected with the dicistronic constructs described in (**a**) and the expression of the different constructs was analysed as in Figure 2C. The lower panel corresponds to a longer exposure of the blot to reveal the CUG-initiated MycCAT form. The figure is representative of at least three independent experiments. (**c**) Total RNA of HeLa cells transfected with constructs described in A was purified and analysed by Northern blotting as described under 'Materials and methods' using a ^{32}P-labelled CAT antisense RNA probe. The same amount of RNA was loaded for each sample. Mono P2 corresponds to a previously described monocistronic construct (Nanbru *et al*., 1997). Size standard RNAs (kb) are indicated

translation initiation of Myc-CAT ORFs (CTG and ATG) at a level comparable to the full-length c-*myc* P2 5′ UTR (Figure 3b, lanes 5 and 6). Indeed, B4 promoted Myc-CAT synthesis even in the absence of domain C at a rate of approximately one-fourth of the cap-dependent translation of the first cistron (mean value: 0.22 ± 0.01) (Figure 3b, compare lanes 3 and 5). Domain C by itself has no IRES activity, as translation of the second cistron from BI C construct is negligible as compared to the cap-dependent translation of the first cistron (mean value: 0.06 ± 0.01). These results also suggest that B4 activates internal translation initiation when placed just upstream of c-*myc* initiation codons.

Two former studies reporting the presence of an IRES in c-*myc* mRNAs provided strong evidences excluding the presence of cryptic promoter(s) within c-*myc* P2 5′UTR (Nanbru *et al*., 1997; Stoneley *et al*., 1998). However, to further rule out this possibility, we verified by Northern blot the size of the transcripts derived from the dicistronic constructs used in this study. As shown in Figure 3c, the mRNAs encoded by the different transfected constructs were similarly expressed and migrated as a single band at the expected size. This observation further confirmed that the B4 sequence acts as an IRES.

Mutational analysis of B4

Based on the computational analysis of c-*myc* P2 5′UTR, B4 is folded in a stem-loop structure. We

evaluated the importance of the predicted stem-loop structure and of the nucleotide sequence of B4 for the IRES activity. Therefore, the base-pairing nucleotides in each side of the stem (S1, S2) as well as the loop sequence (L) were mutated separately (see Figure 4a). The influence of these mutations on the IRES activity of B4 was analysed as previously by the dicistronic vector assay. As shown in Figure 4b, independent mutation of each side of the stem or of the loop did not inhibit B4 IRES activity. However, simultaneous mutation of both sides of the stem significantly reduced B4-mediated internal translation initiation (Figure 4c). Altogether, these results indicate that the IRES activity of B4 is mediated by the sequences composing each side of the predicted stem and that only one of the two sequences is necessary to trigger internal initiation of translation. Moreover, this also shows that the potential secondary structure, in which these sequences might be engaged, seems not important as S1 and S2 are promoting internal translation initiation independently.

We then determined whether any of the two sequences was sufficient to promote IRES activity. Therefore, we generated dicistronic constructs containing S1 or S2 combined to the inactive domain C in the intercistronic region (Figure 5a). The insertion of domain C in the intercistronic region ensured a minimal length between both cistrons to avoid reinitiation events. As shown in Figure 5b, both S1 and S2 sequences activate internal initiation of translation at a rate of one-fifth and one-fourth of the cap-dependent translation of the first

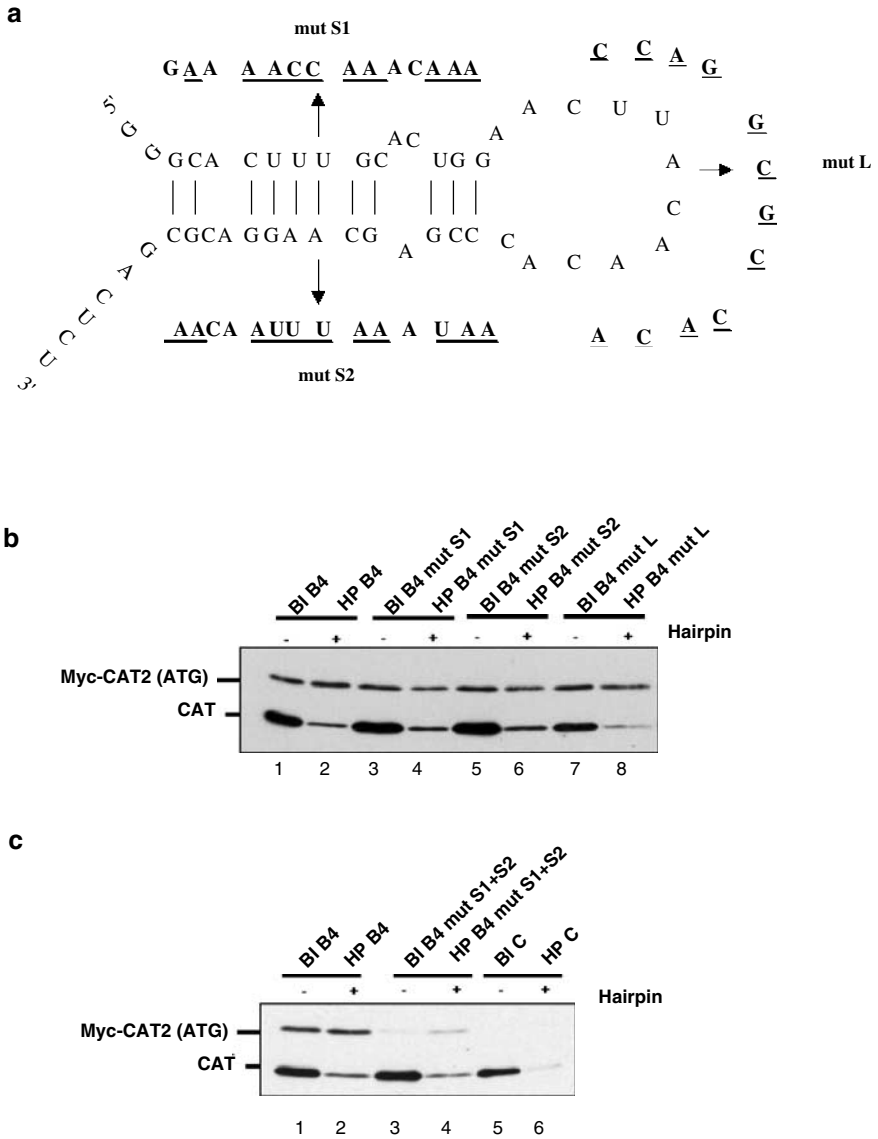

Figure 4 Mutational analysis of B4 sequence. (**a**) Schematic representation of B4 and of the mutated sequences within B4. (**b**) HeLa cells were transfected with the dicistronic constructs containing B4 or mutated versions (mutS1 and mutS2) of B4 described in (**a**). The expression of the different constructs was analysed as described in Figure 2C. (**c**) Analysis of the expression of dicistronic constructs combining mutS1 and mutS2 mutations. The CUG-initiated form is detectable after longer exposure of the blots (data not shown). The figure is representative of at least three independent experiments

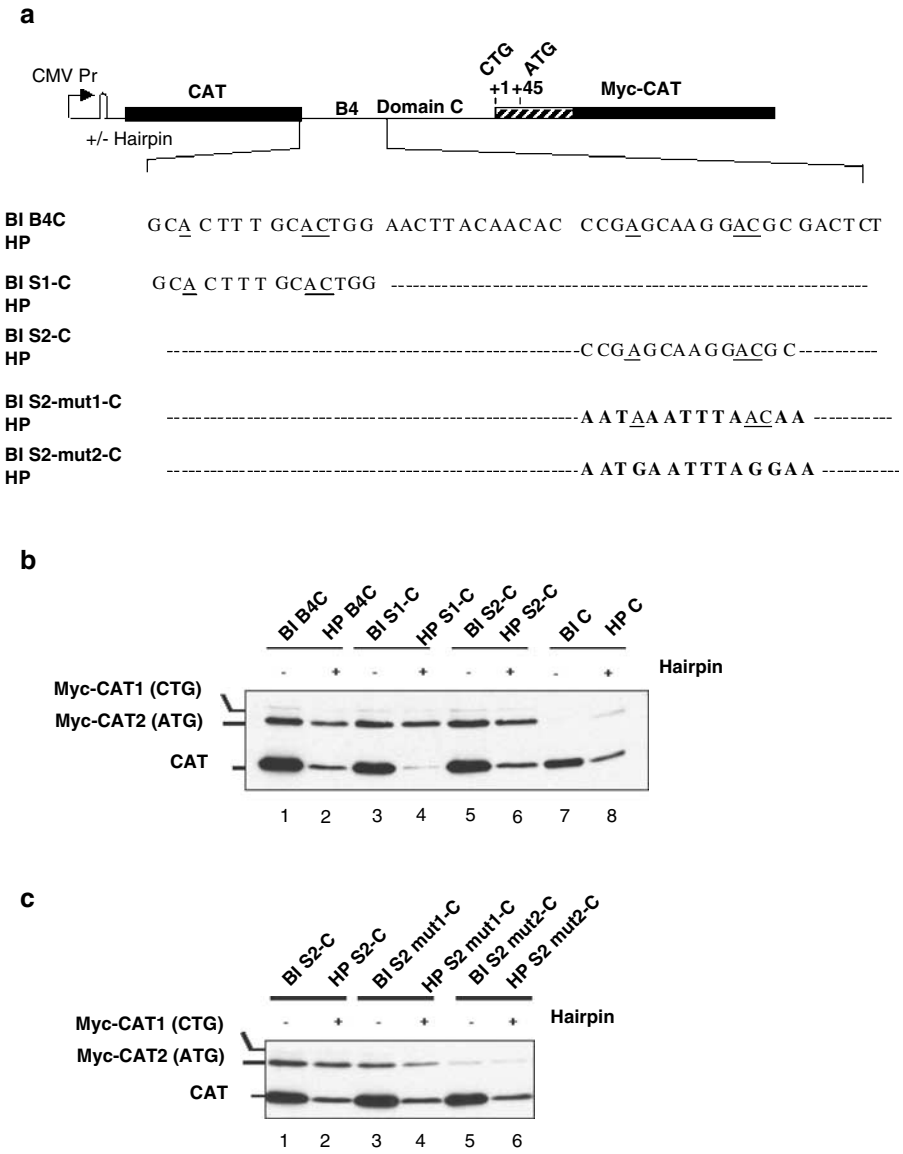

Figure 5 Deletion analysis of B4. (**a**) Schematic representation of the dicistronic DNA constructs used for transfection experiments in (**b** and **c**). B4C was described in Figure 3. S1-C, S2-C contain −143 −130 nt and −117 −104 nt, respectively, of the B4 region fused with the 94-nt C domain. Underlined nucleotides are conserved positions in S1 and S2. Bold nucleotides in S2mut1-C and S2mut2-C correspond to mutated nucleotides. (**b**, **c**) HeLa cells were transfected with the dicistronic constructs described in (**a**) and the expression of the different constructs was analysed as described in Figure 2C. The figure is representative of at least three independent experiments

cistron, respectively (mean values: S1-C: 0.18 ± 0.02, S2-C: 0.28 ± 0.04).

Surprisingly, heavy mutagenesis of S2 sequence except at three positions did not significantly affect IRES activity. However, the additional mutation of these three positions dramatically abolished translation of the second cistron (Figure 5c). It is worth noting that although S1 sequence is very different from S2, it also contains a motif composed of an adenosine residue followed by six nucleotides before an AC doublet.

To rule out the possibility that S1-C or S2-C sequences act as cryptic promoter(s), we inserted these sequences into the pGL2-Basic plasmid allowing the detection of transcriptional activity of DNA sequences by measuring firefly luciferase activity after transfection. This experiment revealed that S1-C and S2-C sequences are unable to confer transcriptional activity to the pGL2-Basic plasmid (data not shown), thereby demonstrating that these sequences mediate internal translation initiation when placed in dicistronic contructs.

B4 recruits the preinitiation complex, which scans the RNA to the AUG/CUG initiation codons

So far, IRES have been described to promote internal initiation according to two different mechanisms. The first one consists of the recruitment and the positioning of the 43S preinitiation complex directly to the initiation

codon. This mechanism was shown to occur for cardiovirus mRNAs. Other IRESes, such as those of enteroviruses and rhinoviruses, recruit the preinitiation complex at an AUG triplet which is not the initiation codon and which is located just downstream the IRES 3′ boundary. The ribosomal complex is then transferred to the downstream AUG initiation codon, probably by a scanning mechanism (for a review, see Jackson and Kaminski, 1995).

The B4 domain of c-*myc* P2 5′ UTR promotes internal initiation at CUG and AUG initiation codons in the presence or the absence of the intervening domain C (Figure 3b). This suggests that B4 might be the ribosome landing site, from which the RNA is scanned until the CUG/ AUG initiation codons. One can assume that while some initiation events occur at the CUG, most preinitiation complexes further scan the RNA to the downstream AUG initiation codon. To verify this hypothesis, we first investigated the influence of the CUG initiation codon and its flanking sequences on B4-mediated internal initiation. As shown in Figure 6, the mutation of the CUG codon to AUU abolished the decoding of Myc-CAT1 ORF without affecting B4-mediated IRES activity on Myc-CAT2 ORF. The same result was obtained upon removal of the sequence from the CUG to the forelast codon before the AUG initiation codon. Furthermore, the replacement of the CUG-AUG intervening sequence by an unrelated sequence did not affect B4 IRES activity. Finally, the IRES activity was maintained upon deletion of the 60 nt downstream from AUG initiation codon. All these observations support the fact that B4 sequence acts as a ribosome landing site from which a scanning process is initiated. To further confirm this mechanism, we determined whether the introduction of a stable hairpin structure (HP′; −60 kcal/mol) just upstream the CUG initiation codon hindered B4-mediated internal initiation. It should be pointed that the HP′ sequence was inserted 88 nt downstream B4 to avoid interference of this element with B4 IRES activity. As control, a sequence of similar length unable to form such a stable secondary structure was also inserted in the dicistronic constructs (see Figure 7a). Whereas the inserted sequence leading to the formation of a stable hairpin structure almost completely abolished internal translation initiation at both CUG and AUG initiation codons, no such effect was observed upon insertion of a nonfolded sequence (Figure 7b). This experiment further supports that B4 sequence recruits the preinitiation complex which then scans the mRNA until the initiation codons are reached.

Discussion

Some viral and cellular mRNAs use IRESes to initiate translation in a cap-independent manner. While viral IRESes participate in a mechanism aimed at the misappropriation of the cellular translational machinery from cellular mRNAs, cellular IRESes allow the expression of certain mRNAs in conditions in which cap-dependent translation initiation is severely impaired. RNA conformation is thought to be critical for the activity of several viral and cellular IRESes (Kaminski *et al*., 1990; Galy *et al*., 2001; Mitchell *et al*., 2003). Here, we show that c-*myc* P2 mRNA 5′UTR is predicted to fold in a Y-shaped secondary structure characteristic of viral IRESes (Le *et al*., 1996) (Figure 1). However, the mapping of c-*myc* P2 5′UTR revealed that internal initiation of translation is actually mediated by a short 50-nt element, named here as B4. Moreover, further dissection of this element allowed the identification of two even shorter sequences of 14 nt, which independently from each other mediate internal translation initiation. c-*myc* mRNA thus constitutes beside *Gtx* mRNA (Chappell *et al*., 2000) the only other example of cellular mRNA whose internal initiation of translation depends on very short sequence elements. These sequences differ significantly and S2 can be extensively mutated without losing its IRES activity. A remarkable exception is the mutation of three nucleotide positions which markedly reduced internal initiation of the second cistron and which are also found in S1 (Figure 5). This common motif might thus play an important role for both S1 and S2 IRES elements. In this regard, it should be mentioned that these nucleotide positions are very conserved between species (Le Quesne *et al*., 2001). Moreover, the screening of libraries of random oligonucleotides for IRES activity led to the identification of a 15-nt sequence also containing an adenosine followed by 6 nts and a AC pair (Owens *et al*., 2001).

Previous mapping of c-*myc* IRES by deletion analysis (Stoneley *et al*., 1998) indicated that internal initiation required a large portion of the c-*myc* 5′UTR. Although the reason for the discrepancy between their data and ours remains unclear, the experimental approaches differ significantly. In our study, we designed CAT-Myc-CAT dicistronic constructs allowing the direct measurement of the expression products of both cistrons in exactly the same experimental conditions. This approach provides a reliable comparison between cap-dependent and IRES-dependent translation initiation on the same RNA molecule as well as an internal control of transfection efficiency. Moreover, the IRES-mediated expression of the second cistron was measured from constructs containing or not a hairpin structure upstream the first cistron. The other study was based on the use of dicistronic constructs from which the level of expression of both cistrons is not directly comparable. Moreover, it lacked control constructs containing a 5′ hairpin structure to ensure the measurement of true internal initiation events.

Our study also reveals that the two short sequences S1 and S2 recruit the 43S preinitiation complex, which then scans the RNA until the AUG or CUG initiation codon. This mechanism is indeed supported by several observations. First, B4 domain promotes internal initiation at CUG and AUG initiation codons of c-*myc* ORFs in the presence or the absence of the intervening domain C (Figure 3b). Second, the disruption of the CUG codon abolished the decoding of Myc-CAT1 ORF without affecting B4-mediated IRES activity on Myc-CAT2

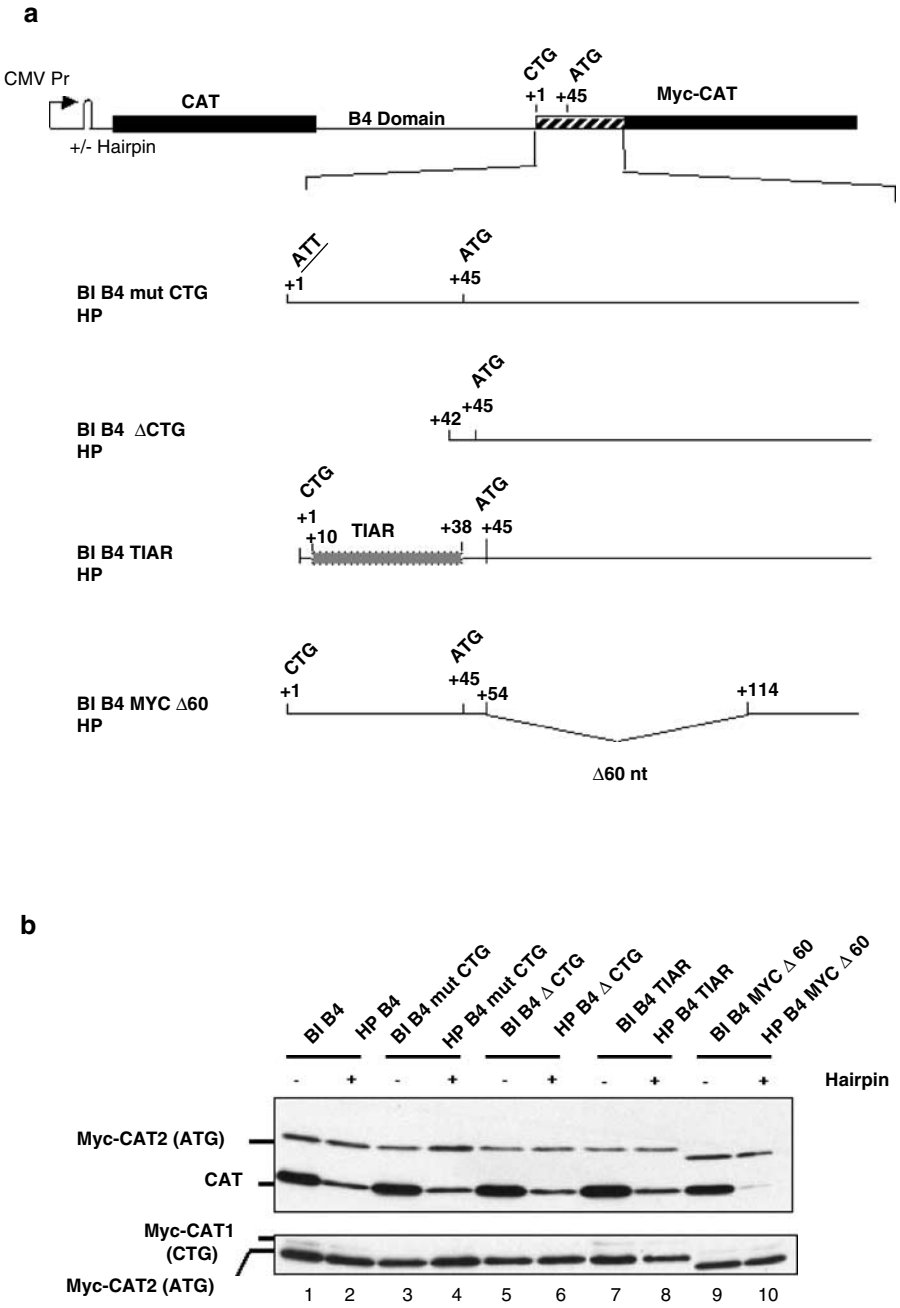

Figure 6 Role of the CUG initiation codon and flanking sequences on B4-mediated internal initiation of translation. (**a**) Schematic representation of the dicistronic DNA constructs used for transfection experiments in (**b**). B4 mut CTG, B4 ΔCTG, B4 TIAR and B4 MYC Δ60 correspond to the B4 region with mutation of the CUG initiation codon (sequence underlined), +1 to +42 nt deletion, replacement of +10 to +38 nt by TIAR coding sequence (gray box) and +54 to +114 nt deletion, respectively. (**b**) HeLa cells were transfected with the dicistronic vectors described in (**a**) and the expression of the different constructs was analysed as in Figure 2C. The lower panel corresponds to a longer exposure of the blot to reveal the CUG-initiated MycCAT form. The figure is representative of at least three independent experiments

ORF. The same results were obtained upon removal of the sequence from the CUG to the AUG initiation codon or upon the replacement of this sequence by an unrelated coding sequence (Figure 6). Finally, the insertion of a stable hairpin structure between B4 and the CUG initiation codon dramatically impairs translation initiation of Myc-CAT ORFs (Figure 7).

Different studies indicate that *Gtx* 9-nt IRES recruits the 40S ribosomal subunit by base pairing to the 18S rRNA (Hu *et al*., 1999; Chappell *et al*., 2000). The c-*myc* IRES modules do not display any homology with *Gtx* 9-nt IRES. Moreover, alignment of c-*myc* IRES modules with human 18S rRNA does not reveal any complementary regions. Therefore, the mechanism by which B4

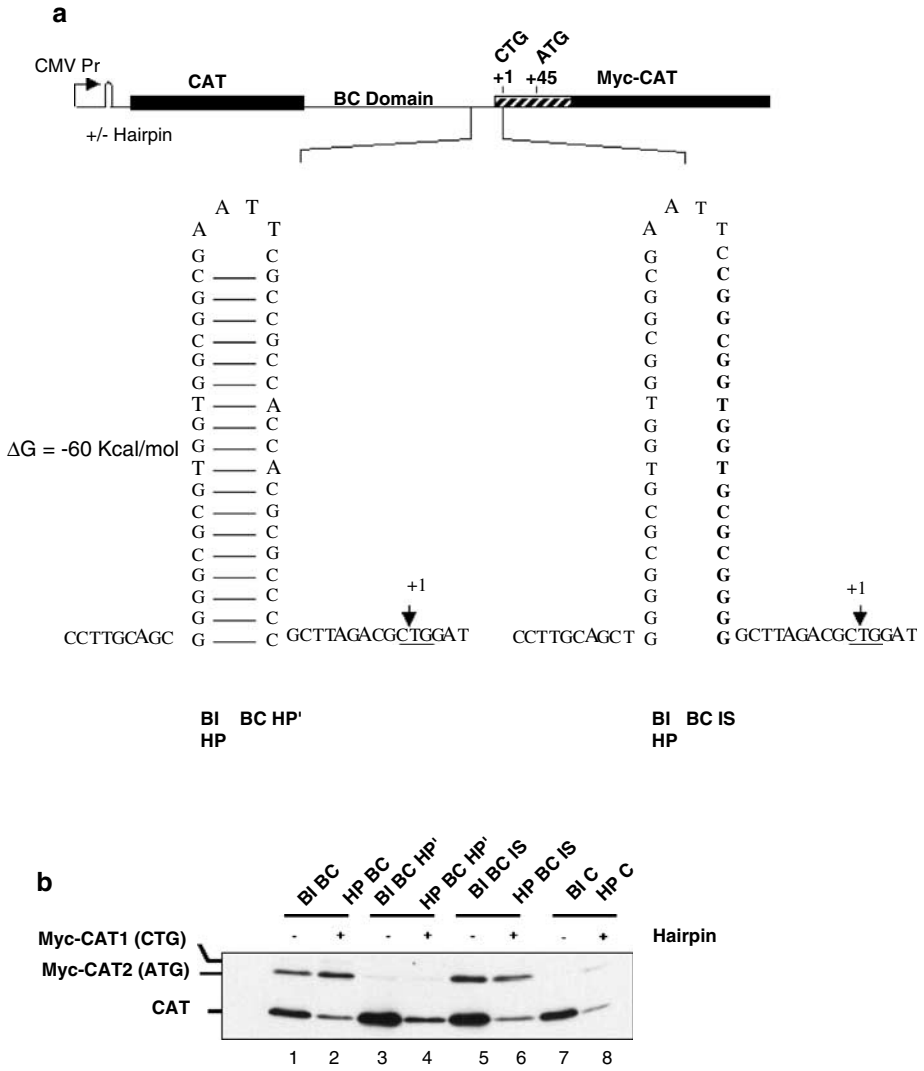

Figure 7 Blocking of B4-mediated internal initiation of translation by insertion of stable hairpin between B4 and the initiation codons. (**a**) Schematic representation of the dicistronic DNA constructs used for transfection experiments in (**b**). BC (or ΔA) was described in Figure 2. BC HP′ contains a hairpin ($\Delta G = -60$ kcal/mol) inserted at position −10 nt. BC IS contains a control sequence corresponding to a nonfolded sequence inserted at the same position. (**b**) HeLa cells were transfected with the dicistronic vectors described in (**a**) and the expression of the different constructs was analysed as in Figure 2C. The figure is representative of at least two independent experiments

sequence modules recruit the 40S ribosomal subunit remains an open question.

It is now well established that internal initiation mediated by most IRESes requires noncanonical translation initiation factors. For example, it has been demonstrated that *xiap* IRES requires La (Holcik and Korneluk, 2000) and hnRNP C (Holcik *et al*., 2003) for activity, while the *Apaf-1* IRES requires upstream of N-ras (unr) and polypyrimidine tract binding protein (PTB) for function (Mitchell *et al*., 2001, 2003). Recently, hnRNP C was reported to increase c-*myc* IRES activity during the G2/M phase by interacting with the heptameric U sequence located between the CUG and AUG initiation codons (Kim *et al*., 2003). However, no other factor promoting constitutive c-*myc* IRES activity has been identified so far. In this regard, complementation of a reticulocyte lysate, in which c-*myc* IRES is poorly active, by purified PTB and unr proteins does not activate c-*myc* IRES (Cencig *et al*., unpublished data).

Factors binding c-*myc* B4 sequence are currently under investigation.

Materials and methods

Plasmid constructions

The constructs Bi/HP P2, Δ2 (renamed here as C), NRS were previously described (Nanbru *et al*., 1997, 2001). Briefly, the BI/HP plasmids are dicistronic constructs containing a variable intercistronic region between the two ORFs (CAT and Myc-CAT) under the control of the cytomegalovirus (CMV) promoter. The chimeric Myc-CAT protein is encoded by a fusion of the 143 first nucleotide of Myc ORF followed by

the CAT coding sequence. The series of HP dicistronic constructs are identical to the BI series except for the presence of hairpin (−40 kcal/mol) upstream CAT ORF. In all the constructs, the 3′ intron region was deleted by a *Bgl*II cleavage. The different constructs were generated by inserting various PCR amplified products corresponding to different regions of c-*myc* P2 5′UTR. These PCR products were introduced in the pSCT monocistronic plasmid (derived from pFC1, Prats *et al*., 1992) in the *Xba*I/*Hin*dIII sites located upstream the CAT sequence. The dicistronic constructs were then generated by inserting the *Xba*I–*Sst*I fragment (variable 5′ region fused to Myc-CAT) derived from the monocistronic pSCT constructs downstream the CAT ORF of BI or HP vectors. The pSCT Δ(A), B4C, S1-C, S2-C, S2 mut1-C and S2 mut2-C were generated by PCR on plasmid pSCT P2 using oligonucleotides O412 (5′-ACGTGATCCCTCTAGAGCTGCGCTGCGGGCGTCCTG-3′)/O413 (5′-ACGTGATCCCAAGCTTGATATCCTCGCTGGGCGCCGG-3′), O874 (5′-ACGTGATCCCTCTAGAGCACTTTGCACTGGAACTTA-3′)/O413, O1376 (5′-GCTCTAGAGCACTTTGCACTGGCCCGACGCGGGGAGGCTATTCTGC-3′)/O413, O1420 (5′-GCTCTAGACCGAGCAAGGACGCCCCGACGCGGGGAGGCTATTCTGC-3′)/O413, O1421 (5′-GCTCTAGAAATAAATTTAACAACCCGACGCGGGGAGGCTATTCTGC-3′)/O413, O1422 (5′-GCTCTAGAAATGAATTTAGGAACCCCGACGCGGGGAGGCTATTCTGC-3′)/O413, respectively. pSCT P2 mutS2 , pSCT P2 mutL, Δ(B1B2B3), Δ(B4) and Δ(C1C2) were generated by a two-step PCR amplification. First, two independent PCR (PCRA and PCRB) fragments corresponding to the regions flanking the deleted sequence were generated using pSCT P2 plasmid as DNA template. A third PCR amplification was performed by combining PCRA and PCRB fragments and external oligonucleotides O414 and O413 to generate the different deletion constructs. The primers used for each construct are specified below. pSCT P2 mutS2: PCRA O414 (5′-ACGTGATCCCTCTAGAACTCGCTGTAGTAATTCCAGCGAGA-3′)/O876 (5′-TCCCCGCGTCGGGAGAGTCTTGTTAAATTTATTGTGTTGTAAGTTCCAGTGCAAA-3′), PCRB O875 (5′-TTTGCACTGGAACTTACAACACAATAAATTTAACAAGACTCTCCCGACGCGGGGA-3′)/O413; P2 mutL: PCRA O414/O878 (5′-GGGAGAGTCGCGTCCTTGCTCGGTGTGGCGCCTGGCCAGTGCAAAGTGCCCGCCC-3′), PCRB O877 (5′-GGGCGGGCACTTTGCACTGGCCAGGCGCCACACCGAGCAAGGACGCGACTCTCCC-3′)/O413; Δ(B4): PCRA O414/O418 (5′-CCGCCCGCTGCTATGGGCAAA-3′), PCRB O417 (5′-CCCATAGCAGCGGGCGGCGACGCGGGGAGGCTATTCT-3′)/O413; Δ(B1B2B3): PCRA O414/O415, PCRB O419 (5′-GGAAGAGCCGGGCGAGCAGAGCACTTTGCACTGGAACTTAC-3′)/O413; Δ(C1C2): PCRA O414/O420 (5′-GGAGAGTCGCGTCCTTGCTCG-3′), PCRB O421 (5′-AGCAAGGACGCGACTCTCCGCAGCTGCTTAGACGCTGGAT-3′)/O413. The pSCT B4, B4ΔCTG, B4mutCTG were generated by a two-step PCR amplification. PCRA was performed by using pSCT P2 as template with primers O874/O1151 (5′-AGAGTCGCGTCCTTGTTCGGGTGTTGTAAGTTC-3′), and PCRB with pSCTΔ2 and primers O1340 (5′-CCGAACAAGGACGCGACTCTACGCTGGATTTTTTCGGGGTAGTG-3′)/O413, O1341 (5′-CCGAACAAGGACGCGACTCTACGATGCCCCTCAACGTTAGCTT-3′)/O413, O1298 (5′-CCGAACAAGGACGCGACTCTGATTGATTTTTTTCGGGTAGTGGAA-3′)/O413, respectively. PCRA and PCRB were combined in a third PCR with primers O874/O413. The pSCT B4 mutS1 was generated by PCR amplification of pSCT B4 using oligonucleotides O1211 (5′-GCTCTAGAGAAAACCAAACAAAAACTTACAACACCCGAGCAAGGAC-3′)/O413.

The pSCT B4 mutS2 was obtained by a two-step PCR amplification. PCRA was performed with pSCT P2 mutS2 as template with primers O874/O1215 (5′-AGAGTCGTTTTAAATTTATTGTGT-3′), PCRB was performed using pSCT Δ2 with primers O1418 (5′-AATAAATTTAAAACGACTCTACGCTGGATTTTTTTCGGGTAGTGGA-3′)/O413. PCRA and PCRB were combined (PCRC) with primers O874/O413. The pSCT B4 mutS1 + S2 was obtained by PCR amplification of pSCT B4mutS2 using primers O1214 (5′-GCTCTAGAGAAAACCAAACAAAAACTTACAACACAATAAATTTAAC-3′)/O413.

The pSCT B4 mutL was obtained by a two-step PCR amplification. PCRA was performed by using pSCT P2 mutL as template with primers O1180 (5′-GCTCTAGACACTTTGCACTGGCCAGGCG-3′)/O1213 (5′-AGAGTCGCGTCCTTGTTCGGTGT-3′) and PCRB using pSCT Δ2 and primers O1419 (5′-CCGAACAAGGACGCGACTCTACGCTGGATTTTTTTCGGGTAGTGGAA-3′)/O413. PCRA and PCRB were combined (PCRC) with primers O1180/O413. The pSCT B4TIAR and B4 MYCΔ60 were obtained by a two-step PCR amplification: PCRA with pSCT B4 and primers O874/ O1426 (5′-GACGGAGTGATCCCGGGACAAGGGGGAGGGCAGCGTAGAGTCGCGTCCTTGTTC-3′) and O874/O1344 (5′-GAGGGGCATCGTCGCGGGAGGTTG-3′), PCRB with pSCTΔ2 with primers O1331 (5′-TCCCGGGATCACTCCGTCGCACCCGCGACGATGCCCCTCAACGTTAGC-3′)/O413 and O1346 (5′-CCTCCCGCGACGATGCCCCTCCACTGCGACGAGGAGGAGAACTTC-3′)/O413. PCRA and PCRB were combined (PCRC) with primers O874/O413. The pSCT BC HP′ and BC IS were obtained by a two-step PCR amplification: PCRA with pSCT P2 and primers O412/ O1366 (5′-GAATTCGCCGCCACCACGCGCCCCAGCTGCAAGGAGAGCCTTTCAG-3′) and O412/O1402 (5′-CCGAATTCGCCGCCACCACGCGCCCCAGCTGCAAGGAGAGCCTTTCAG-3′), PCRB with pSCTΔ2 with primers O1367 (5′-CGTGGTGGCGGCGAATTCGCCGCCACCACGCGCCCCGCTTAGACGCTGGATTTTTTT-3′)/O413 and O1403 (5′-CGTGGTGGCGGCGAATTCGGGGCGCGTGGTGGCGGCGCTTAGACGCTGGATTTTTTT-3′)/O413. PCRA and PCRB were combined (PCRC) with primers O412/O413.

DNA transfection, Western immunoblotting and quantification of Western blots HeLa cells were grown in DMEM 10% fetal calf serum (Life Technologies) and were transfected using the Fugene-6 transfection reagent (Roche) according to the manufacturer's instructions (1 μg of DNA). At 24 h after transfection, cell lysate was prepared and used for Western immunoblotting as previously described (Vagner *et al*., 1995). For quantification, the DNA constructs were transfected in triplicate. The expression of the two cistrons was analysed by Western blot, followed by the quantification of the chemiluminescent signals using a CCD camera (AlphaInnotec). The mean values correspond to the Myc-CAT/CAT ratios.

RNA extraction and Northern blotting Total cellular RNA was prepared by the Trizol method (Life Technologies), according to the manufacturer's instructions. The quality of the RNA samples was verified by agarose gel electrophoresis. A measure of 3 μg of total RNA was loaded on a 1.5% agarose gel and Northern blot was performed as described (Kruys *et al*., 1993). CAT antisense RNA probes were generated by *in vitro* transcription using the T7 Maxiscript kit (Ambion) according to the manufacturer's instructions, using a linearized DNA template in the presence of 80 μCi [α-^{32}P]UTP (800 Ci/mmol) and 20 μM UTP.

Acknowledgements
We thank Dr Louis Droogmans for helpful discussions and for revising the manuscript. This work was funded by the EC contract (QLK3-2000-00721), the Fund for Medical Scientific Research (Belgium, Grant 3.4618.01) and the 'Actions de Recherches Concertées' (Grant 00-05/250). S Cencig is supported by an FRIA grant (Belgium).

References

Akiri G, Nahari D, Finkelstein Y, Le SY, Elroy-Stein O and Levi BZ. (1998). *Oncogene,* **17,** 227–236.
Bentley DL and Groudine M. (1986a). *Nature,* **321,** 702–706.
Bentley DL and Groudine M. (1986b). *Mol. Cell. Biol.,* **6,** 3481–3489.
Bernstein J, Sella O, Le SY and Elroy-Stein O. (1997). *J. Biol. Chem.,* **272,** 9356–9362.
Blackwood EM, Lugo TG, Kretzner L, King MW, Street AJ, Witte ON and Eisenman RN. (1994). *Mol. Biol. Cell,* **5,** 597–609.
Chappell SA, Edelman GM and Mauro VP. (2000). *Proc. Natl. Acad. Sci. USA,* **97,** 1536–1541.
Cornelis S, Bruynooghe Y, Denecker G, Van Huffel S, Tinton S and Beyaert R. (2000). *Mol. Cell,* **5,** 597–605.
Creancier L, Mercier P, Prats AC and Morello D. (2001). *Mol. Cell. Biol.,* **21,** 1833–1840.
Galy B, Créancier L, Prado-Lourenco L, Prats AC and Prats H. (2001). *Oncogene,* **20,** 4613–4620.
Hann SR, Dixit M, Sears RC and Sealy L. (1994). *Genes Dev.,* **8,** 2441–2452.
Hann SR, King MW, Bentley DL, Anderson CW and Eisenman RN. (1988). *Cell,* **52,** 185–195.
Hann SR, Sloan-Brown K and Spotts GD. (1992). *Genes Dev.,* **6,** 1229–1240.
Henis-Korenblit S, Strumpf NL, Goldstaub D and Kimchi A. (2000). *Mol. Cell. Biol.,* **20,** 496–506.
Holcik M, Gordon BW and Korneluk RG. (2003). *Mol. Cell. Biol.,* **23,** 280–288.
Holcik M and Korneluk RG. (2000). *Mol. Cell. Biol.,* **20,** 4648–4657.
Holcik M, Lefebvre C, Yeh C, Chow T and Korneluk RG. (1999). *Nat. Cell Biol.,* **1,** 190–192.
Hu MC, Tranque P, Edelman GM and Mauro VP. (1999). *Proc. Natl. Acad. Sci. USA,* **96,** 1339–1344.
Huez I, Creancier L, Audigier S, Gensac MC, Prats AC and Prats H. (1998). *Mol. Cell. Biol.,* **18,** 6178–6190.
Jackson RJ. (1988). *Nature,* **334,** 292–293.
Jackson RJ and Kaminski A. (1995). *RNA,* **1,** 985–1000.
Johannes G, Carter MS, Eisen MB, Brown PO and Sarnow P. (1999). *Proc. Natl. Acad. Sci. USA,* **96,** 13118–13123.
Johannes G and Sarnow P. (1998). *RNA,* **4,** 1500–1513.
Kaminski A, Howell MT and Jackson RJ. (1990). *EMBO J.,* **9,** 3753–3759.
Kim JH, Paek KY, Choi K, Kim TD, Hahm B, Kim KT and Jang SK. (2003). *Mol. Cell. Biol.,* **23,** 708–720.
Kruys V, Thompson P and Beutler B. (1993). *J. Exp. Med.,* **177,** 1383–1390.
Le SY and Maizel Jr JV. (1997). *Nucleic Acids Res.,* **25,** 362–369.
Le SY, Siddiqui A and Maizel Jr JV. (1996). *Virus Genes,* **12,** 135–147.
Le Quesne JPC, Stoneley M, Fraser A and Willis A. (2001). *J. Mol. Biol.,* **310,** 111–126.
Marcu KB, Bossone SA and Patel AJ. (1992). *Annu. Rev. Biochem.,* **61,** 809–860.
Mathews DH, Sabina J, Zuker M and Turner DH. (1999). *J. Mol. Biol.,* **288,** 911–940.
Mitchell SA, Brown EC, Coldwell MJ, Jackson RJ and Willis AE. (2001). *Mol. Cell. Biol.,* **21,** 3364–3374.
Mitchell SA, Spriggs KA, Coldwell MJ, Jackson RJ and Willis AE. (2003). *Mol. Cell,* **11,** 757–771.
Nanbru C, Lafon I, Audigier S, Gensac MC, Vagner S, Huez G and Prats AC. (1997). *J. Biol. Chem.,* **272,** 32061–32066.
Nanbru C, Prats AC, Droogmans L, Defrance P, Huez G and Kruys V. (2001). *Oncogene,* **20,** 4270–4280.
Obaya AJ, Mateyak MK and Sedivy JM. (1999). *Oncogene,* **18,** 2934–2941.
Owens GC, Chappell SA, Mauro VP and Edelman GM. (2001). *Proc. Natl. Acad. Sci. USA,* **98,** 1471–1476.
Pelletier J and Sonenberg N. (1988). *Nature,* **334,** 320–325.
Prats AC, Vagner S, Prats H and Andrie F. (1992). *Mol. Cell. Biol.,* **12,** 4796–4805.
Pyronnet S, Pradayrol L and Sonenberg N. (2000). *Mol. Cell,* **5,** 607–616.
Ryan KM and Birnie GD. (1996). *Biochem. J.,* **314** (Part 3)**,** 713–721.
Sella O, Gerlitz G, Le SY and Elroy-Stein O. (1999). *Mol. Cell. Biol.,* **19,** 5429–5440.
Spencer CA, LeStrange RC, Novak U, Hayward WS and Groudine M. (1990). *Genes Dev.,* **4,** 75–88.
Stoneley M, Chappell SA, Jopling CL, Dickens M, MacFarlane M and Willis AE. (2000). *Mol. Cell. Biol.,* **20,** 1162–1169.
Stoneley M, Paulin FE, Le Quesne JP, Chappell SA and Willis AE. (1998). *Oncogene,* **16,** 423–428.
Subkhankulova T, Mitchell SA and Willis AE. (2001). *Biochem. J.,* **359,** 183–192.
Teerink H, Voorma HO and Thomas AA. (1995). *Biochim. Biophys. Acta,* **1264,** 403–408.
Vagner S, Gensac MC, Maret A, Bayard F, Amalric F, Prats H and Prats AC. (1995). *Mol. Cell. Biol.,* **15,** 35–44.
Willis AE. (1999). *Int. J. Biochem. Cell Biol.,* **31,** 73–86.